Pharm Res (2015) 32:852–862
DOI 10.1007/s11095-014-1501-5

RESEARCH PAPER

Pharmacokinetics, Antitumor and Cardioprotective Effects of Liposome-Encapsulated Phenylaminoethyl Selenide in Human Prostate Cancer Rodent Models

Jeong Yeon Kang • Mathew Eggert • Shravanthi Mouli • Ibrahim Aljuffali • Xiaoyu Fu • Ben Nie • Amy Sheil • Kendall Waddey • Charlie D. Oldham • Sheldon W. May • Rajesh Amin • Robert D. Arnold

Received: 24 April 2014 / Accepted: 20 August 2014 / Published online: 27 August 2014

ABSTRACT

Purpose Cardiotoxicity associated with the use of doxorubicin (DOX), and other chemotherapeutics, limits their clinical potential. This study determined the pharmacokinetics and antitumor and cardioprotective activity of free and liposome encapsulated phenyl-2-aminoethyl-selenide (PAESe).

Methods The pharmacokinetics of free PAESe and PAESe encapsulated in liposomes (SSL-PAESe) were determined in rats using liquid chromatography tandem mass-spectrometry. The antitumor and cardioprotective effects were determined in a mouse xenograft model of human prostate (PC-3) cancer and cardiomyocytes (H9C2).

Results The encapsulation of PAESe in liposomes increased the circulation half-life and area under the drug concentration time profile, and decreased total systemic clearance significantly compared to free PAESe. Free- and SSL-PAESe improved survival, decreased weight-loss and prevented cardiac hypertrophy significantly in tumor bearing and healthy mice following treatment with DOX at 5 and 12.5 mg/kg. *In vitro* studies revealed PAESe treatment altered formation of reactive oxygen species (ROS), cardiac hypertrophy and gene expression, *i.e.,* atrial natriuretic peptide and myosin heavy chain complex beta, in H9C2 cells.

Conclusions Treatment with free and SSL-PAESe exhibited antitumor activity in a prostate xenograft model and mitigated DOX-mediated cardiotoxicity.

KEY WORDS cardiotoxicity · doxorubicin · liposomes · phenylaminoethyl selenide · prostate cancer

ABBREVIATIONS

ACN	Acetonitrile
ANP	Atrial natriuretic peptide
AUC	Area under the plasma drug concentration-time curve
Chol	Cholesterol
CL	Total systemic clearance
C_{max}	Maximum plasma concentration
CV	Coefficient of variation
DOX	Doxorubicin
DSPC	1,2-distearoyl-sn-glycero-3-phosphatidylcholine
DSPE-PEG	1,2-distearoyl-sn-glycero-3-phosphoethanolamine-N-[methoxy(polyethylene glycol)-2000]
ESI	Electrospray ionization
FPAESe	4-fluoro-phenyl-2-aminoethyl selenide
H_2DCFDA	2′-7′- dichlorodihydrofluorescein diacetate
I.S.	Internal standard
k	Terminal elimination rate
LC	High performance liquid chromatography

Electronic supplementary material The online version of this article (doi:10.1007/s11095-014-1501-5) contains supplementary material, which is available to authorized users.

J. Y. Kang • I. Aljuffali
Department of Pharmaceutical and Biomedical Sciences, College of Pharmacy, University of Georgia, Athens, Georgia 30602, USA

M. Eggert • S. Mouli • X. Fu • B. Nie • A. Sheil • K. Waddey • R. Amin • R. D. Arnold (✉)
Department of Drug Discovery & Development, Harrison School of Pharmacy, Auburn University, Walker Building, Room 3211-D, Auburn Alabama 36849, USA
e-mail: rda0007@auburn.edu

C. D. Oldham • S. W. May
School of Chemistry & Biochemistry, Georgia Institute of Technology, Atlanta, Georgia 30332, USA

Present Address:
I. Aljuffali
Nanomedicine Research Unit, Department of Pharmaceutics, College of Pharmacy, King Saud University, Riyadh, Saudi Arabia

Lip-PAESe	SSL-PAESe
LLOQ	Lower limit of quantification
m/z	Mass to charge
MeOH	Methanol
MHC-β	Myosin heavy chain complex beta
MRM	Multiple reaction monitoring
MS	Mass spectrometry
MS/MS	Tandem mass spectrometry
PAESe	Phenyl-2-aminoethyl selenide
PK	Pharmacokinetic
QC	Quality control
qPCR	Quantitative polymerase chain reaction
ROS	Reactive oxygen species
sc	Subcutaneous
SSL	Sterically-stabilized liposomes
SSL-PAESe	Sterically stabilized PAESe liposomes
$t_{1/2}$	Half-life
V	Apparent volume of distribution
$\alpha_{t1/2}$	Alpha distribution half-life
$\beta_{t1/2}$	Beta elimination half-life

INTRODUCTION

Doxorubicin (DOX) is a potent anticancer agent used to treat primary and metastatic malignancies, *i.e.*, acute leukemia, non-Hodgkin's lymphomas, breast, ovarian and lung cancer (1). However, the clinical usage of DOX and other anthracyclines are limited, in part, by myocardial damage resulting from generation of reactive free radicals such as superoxide anion, hydroxyl radical and peroxynitrite (2, 3). A variety of scavenging and antioxidant agents have been explored as chemoprotectants with the goal of reducing oxidative damage and alleviating DOX-mediated cardiotoxicity. Antioxidants, such as dexrazoxane (Zinecard®) and amifostine (Ethyol®), are used clinically to decrease free radical-associated toxicity of chemotherapeutics, such as DOX and cisplatin. As a potent iron chelator, dexrazoxane interrupts free radical generation induced by anthracycline-iron complexation (4, 5). However, dexrazoxane has been shown to reduce the antitumor activity of chemotherapeutic agents and displays unwanted side effects, such as acute myeloid leukemia and myelosuppression, which have limited its usefulness (4, 5). Amifostine has been shown to reduce the toxicity of platinum-based drugs, such as cisplatin, on the kidney and the salivary glands, but was less cardioprotective than dexrazoxane following treatment with DOX, and didn't improve weight loss and mortality in a spontaneously hypertensive rat model (4, 6, 7). Failure to achieve sufficient chemotherapeutic drug exposure to eradicate primary and/or metastatic disease, can lead to drug resistance, disease recurrence and death. Earlier detection of cancers combined with more aggressive treatment protocols have resulted in increased rates of survival and longer remission times for many cancers. Therefore, there is a clinical need to have greater flexibility in dosing DOX without risks associated with cardiotoxicity.

Phenyl-2-aminoethyl selenide (PAESe, Fig. 1b) is a selenium-containing antioxidant that exerts its activity by reacting with metabolic oxidants such as peroxide, peroxynitrite anion and hydroperoxides using selenium redox recycling (8–11). Previously, we demonstrated that PAESe had a protective effect against DOX-induced cardiotoxicity using *in vitro* and *in vivo* mouse models of human prostate (PC-3) cancer (12). In that study, the growth inhibitory effects of DOX were not altered by PAESe (up to 10 μM) on PC-3 cells *in vitro*, and PAESe decreased formation of intracellular reactive free radicals from DOX in a dose-dependent manner. Most interestingly, findings from that study suggested that PAESe exerted antitumor activity in an *in vivo* human prostate adenocarcinoma (PC-3) tumor xenograft mouse model; however this observation and the mechanism(s) of this effect were not clear and required further examination (12).

The objectives of this study were to encapsulate PAESe in a lipid-based, *i.e.,* liposome, nanoparticulate drug carrier and determine the systemic pharmacokinetics, and examine the antitumor and cardioprotective activity of free- and liposome encapsulated-PAESe. A sensitive and selective high-performance liquid chromatography—tandem mass spectrometry (LC-MS/MS) assay with electrospray ionization (ESI) was developed and used to quantify PAESe in small volume rat plasma samples. This assay was used to quantify and determine the effect of encapsulating PAESe in liposomes on its disposition, *e.g.,* circulation half-life and systemic drug exposure (AUC), in rats.

PAESe was encapsulated in sterically-stabilized liposomes (SSL-PAESe) to support mechanistic and therapeutic studies to determine the effect of drug exposure on PAESe activity. Nanoparticulate drug carriers such as sterically stabilized liposome are known to alter drug disposition, *i.e.,* circulation half-life, tissue/tumor distribution and rate/extent of drug release (13–16). DOX encapsulated in sterically stabilized liposomes is approved in the U.S. (Doxil®), Canada (Caelyx®) and abroad. These formulations have been shown to enhance antitumor activity and reduced cardiotoxicity (13, 17, 18). Although DOX, daunorubicin and other anthracyclines have been encapsulated within liposomes and show reduced cardiotoxicity, the use of free - unencapsulated - drug remains the most prevalent clinically utilized form and cardiotoxicity remains a primary limitation in their effective use.

The antitumor and cardioprotective activities of PAESe were investigated *in vivo* using a healthy and an established human prostate (PC-3) tumor xenograft model in athymic NCr (*nu/nu*) nude mice. Previous studies showed that PAESe

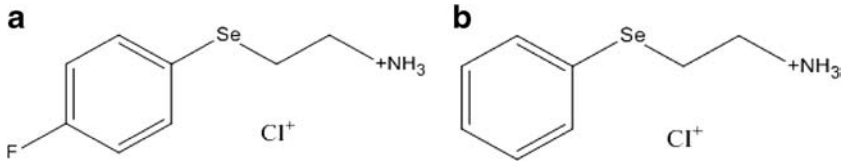

Fig. 1 Chemical structures of phenylaminoalkyl selenide (**a**) 4-fluoro-phenyl-2-aminoethyl selenide (FPAESe), the internal standard (I.S.) and (**b**) phenyl-2-aminoethyl selenide (PAESe).

reduced DOX-mediated neutrophil and macrophage cardio-infiltration when compared to DOX treated animals (12). Surprisingly, tumor growth (volume) from PAESe treated mice was similar to DOX treatment groups. Therefore we hypothesized that encapsulation of PAESe in liposomes would enhance deposition and improve antitumor activity relative to free drug (13–16). This model was used to examine the effect of free and PAESe encapsulated in liposomes on tumor growth and survival. Healthy mice were also used to determine if concomitant administration of PAESe would permit treatment with greater doses of free DOX.

To gain mechanistic insights into the prolonged survival and cardioprotective activity, previously observed (12), *in vitro* studies using rat derived cardiomyocytes (H9C2) cells were used to examine effect of PAESe on DOX-mediated toxicity, generation of reactive oxygen species (ROS) and development of cardiac hypertrophy.

MATERIALS AND METHODS

Materials

Analytical (LC/MS) grade methanol (MeOH), acetonitrile (ACN), formic acid, chloroform and sucrose were obtained from Thermo Fisher Scientific Inc. (Rockford, IL). Phospholipids, 1,2-distearoyl-sn-glycero-3-phosphatidylcholine (DSPC) and 1,2-distearoyl-sn-glycero-3-phosphoethanol-amine-N-[methoxy(polyethylene glycol)-2000] (DSPE-PEG) were purchased from Avanti Polar Lipids Inc., (Alabaster, AL). Cholesterol (Chol) was purchased from Sigma-Aldrich (St. Louis, MO) and recrystallized (×3) from MeOH before use. Ultrapure water (>3 mega Ω) was obtained from a Millipore Milli-Q synthesis system (Billerica, MA). Heparin sodium for injection USP (5,000 units/mL) was purchased from Elkin-Sinn, Inc., (Cherry Hill, NJ). All other chemicals and solvents were of analytical grade and obtained from Sigma-Aldrich (St. Louis, MO).

Preparation of PAESe Liposomes

Sterically stabilized PAESe liposomes (SSL-PAESe) were formulated with DSPC:Chol:DSPE-PEG (9:5:1 lipid mole ratio) by thin-film hydration method and remote loading procedure that is based on the encapsulation of charged drugs into preformed vesicles using combined pH and electrochemical gradients (13, 14, 17–19). Briefly, thin-films were formed by transferring lipids and cholesterol dissolved in chloroform into glass tubes and dried under vacuum (Büchi Rotavapor). Lipid thin-films were hydrated with ammonium sulfate (250 mM, pH 5.0) and were passed through double-stacked polycarbonate filters (0.08 μm, GE Water & Process Tech., Boulder, CO) using a thermo-barrel high-pressure extruder (Northern Lipids, Vancouver, British Columbia, Canada) at 60°C. Unencapsulated ammonium sulfate was removed by repetitive (×3) dialysis against an isotonic sucrose solution (10%, w/v) at 4°C overnight. PAESe solution was mixed with the preformed vesicles with occasional vortexing, and unencapsulated PAESe was removed by membrane dialysis. The final SSL-PAESe formulations were stored at 4°C protected from light and used within 1 week of preparation.

Encapsulation efficiency of formulations was determined by comparing the drug:lipid ratio of the final product to initial concentrations of PAESe and phospholipid (Fig. S1). The concentration of PAESe was determined using a Synergy HT Multi-Mode Microplate Reader at 260 nm (BioTek Instruments Inc., Winooski, VT). The phospholipid concentration was measured using an inorganic phosphate assay following acid hydrolysis (20). Mean particle size of SSL-PAESe was measured using a Nicomp model 380 DLS submicron particle size analyzer (Santa Barbara, CA). A mean diameter (volume weighted) of final SSL-PAESe formulations ranged from 80–110 nM and the final concentration of PAESe was typically 1.5 mg/mL with >80% encapsulation efficiency at a drug:lipid ratio of 0.2:1.0 (mol:mol).

Plasma Pharmacokinetics - Rats

Fisher 344 male rats, 160–200 g, (Harlan Sprague–Dawley, Indianapolis, IN) were anesthetized with 90 mg/kg ketamine and 9 mg/kg xylazine by intramuscular injection into the thigh. The jugular vein was cannulated with polyurethane tubing, which was exteriorized through a scapular incision. Three days after surgery, free PAESe (10 mg/kg) or SSL-PAESe (5 mg/kg) was administered intravenously (*i.v.*) *via* lateral tail vein injection. Blood samples (100–200 μL) were collected *via* a jugular cannula at −10 (baseline), 2, 5, 10, 15, 20, 30, 45 min, 1, 2, 4 h for free PAESe group and −10, 2, 5, 15, 30, 45 min, 1, 2, 4, 6, 8, 12, 24, 48, 120 h for SSL-PAESe group after dosing following a staggered sampling to minimize excessive blood loss, and cooled on ice immediately. Plasma

was collected by centrifugation of blood at 1,200×g for 10 min at 4°C, snap-frozen in liquid nitrogen and stored at −80°C until analysis by liquid chromatography tandem mass spectrometry (LC-MS/MS), described below and supplemental data. Animals were provided a standard rat chow diet and water *ad libitum* and were kept in a light- and temperature-controlled room. All procedures regarding animal handling, care and surgery followed a protocol approved by the Institutional Animal Care and Use Committee (IACUC) of the University of Georgia and Auburn University according to the US Public Health Service (PHS) Policy on Human Care and Use of Laboratory Animals, updated 2002.

LC-MS/MS Analysis

Plasma samples (50 μL) were spiked with internal standard, 4-fluoro-phenyl-2-aminoethyl selenide (FPAESe), mixed with ice-cold ACN (200 μL) and vortexed. Samples were cooled in an ice-water bath for 1 h, centrifuged at 1,200×*g* for 10 min at 4°C. The deproteinized supernatant was dried with a stream of filtered nitrogen and the residues were reconstituted with 100 μL of mobile phase and analyzed by LC-MS/MS (***supplemental data***).

Pharmacokinetic Analysis

A computational model was fit to the observed data and used to predict pharmacokinetic (PK) parameters, *i.e.*, terminal elimination rate (k), half-life ($t_{1/2}$), apparent volume of distribution (V), total systemic clearance (CL) and area under the plasma drug concentration-time curve (AUC), and their precision after free drug and SSL-PAESe administration. Initial parameter estimates for PK modeling were generated using a noncompartmental analysis using (WinNonlin Professional version 5.3, Pharsight Corp., Mountain View, CA). The PK model was fit using naïve-pooled data and naïve-averaged data approaches (21). Residuals, accuracy, precision, confidence intervals, correlation between parameters, condition number and objective criteria (Akaike information criteria, Schwarz criteria, sum of squares, and estimator criterion value) were analyzed to evaluate goodness-of-fit as well as select the best-fit model using WinNonlin (13, 21). Parameter estimates from data for animals treated with each formulation were compared using a student *t*-test. Differences were considered statistically significant at $p<0.05$ using SigmaStat v.3.11 (Systat, San Jose, CA).

Tumor Implantation and Treatment

Prostate Cells

Androgen-independent human prostate epithelial cells (PC-3) were obtained from American Type Culture Collection (Rockville, MD) and were maintained in culture using F-12 K media supplemented with 10% (v/v) FBS in a humidified cell culture chamber (NuAire Inc. Plymouth, MN) at 37°C and 5% CO_2. Cells were passaged when they reached approximately 80–90% confluency.

Animal Model

Athymic, NCr nude (*nu/nu*) mice (body weight, approx. 25 g) at 6–8 weeks of age were obtained from Taconic Farms, Inc., (Germantown, NY). Mice were maintained according to an approved Institutional Animal Care and Use Committee (IACUC) protocols at the University of Georgia and Auburn University, the U.S. Public Health Service (PHS) Policy on Human Care and Use of Laboratory Animals, updated 2002. Mice were kept in pathogen-free cages in a light and temperature-controlled isolated room and provided with standard rodent chow and sterile water *ad libitum* during the experimental periods. A PC-3 cell suspension in serum free media (1×10^7 cells/mL) was mixed with ice-cold Matrigel (BD Biosciences, Franklin Lakes, NJ) in 1:1 (v/v), and 100 μL of the mixture was injected subcutaneously (sc) into the flank of nude mice to establish tumor xenograft. Tumor growth and body weight were monitored every 2–3 days. Tumor volume was estimated manually using digital calipers as described previously where the volume was the product of largest dimension and (smallest dimension)$^2\times0.52$ (22). Treatment was initiated 2 weeks after inoculation of tumor cells when tumor volume reached approximately 200 mm^3. DOX and PAESe were dissolved in normal saline (0.90%, w/v) and sterilized using a 0.2 μm syringe nylon filter. SSL-PAESe was prepared as described above. Mice were divided randomly into 6 groups: DOX, PAESe, DOX + PAESe, SSL-PAESe, DOX + SSL-PAESe, and control (vehicle), $n=8$–10 animals/cohort. Formulations (100 to 150 μL) were administered weekly for 4 weeks (a total of 5 treatments) by lateral tail vein injection; a dose of 5 mg/kg for DOX, 10 mg/kg for PAESe, 5 mg/kg DOX + 10 mg/kg PAESe, 5 mg/kg SSL-PAESe and 5 mg/kg DOX + 5 mg/kg SSL-PAESe. Control groups were treated with normal saline following the same dosing schedule. Tumor growth and body weight were measured every 3 days. Tumor volume was determined as described above. Mice were monitored every day for survival and signs of treatment-mediated toxicity, such as weight loss, bloody stool and reduced activity. Mice were euthanized if weight loss exceeded 20% of their initial body weight—corrected for tumor volume (assuming a density of 1.0 g/cm^3), ulceration of sc-tumor or obvious signs of toxicity such as infection or if lethargy were observed (23). For any animal that was euthanized, death was considered to have happened on the following day. After sacrificing mice by CO_2, the hearts were excised and fixed in formalin solution for histological evaluation. Tumor volume and body weight (mean ± SEM) for each group was plotted against time *versus* tumor volume or body

weight normalized to day 0 (start of treatment). A Kaplan-Meir plot was used to visualize survival data and a Log-rank (Mantel-Cox) test was used determine if treatment-mediated differences in survival were significant, $p<0.05$ (SigmaStat, v.3.11).

Histological Examination—Cardiac Hypertrophy

For histological evaluation, each heart was fixed in formalin solutions (10%, v/v) for 24 h, bisected longitudinally and embedded in paraffin. A total of 9 serial sections, at 100 μm, for each heart were collected and stained with hematoxylin and eosin (H&E). Micrographs, 5 field of views/section × 9 sections/heart, were captured using an Olympus BX51 microscope. Two naïve individuals blinded to treatment measured the cross sectional width of 5 representative cardiomyocytes for each field of view using Image J (v. 1.47). Data were normalized to control cardiomyocytes and analyzed using a one-way ANOVA followed by a post hoc Bonferroni (all pair-wise comparisons) using (SigmaStat, v.3.11). Differences in size were considered significant at $p<0.05$.

Effect of PAESe on Survival with Greater DOX Dosing

To examine the ability to PAESe to reduce cardiotoxicity and permit administration of greater doses of DOX, a survival study in the absence of an implanted tumor was completed in athymic nude NCr mice. Mice were randomized and divided into 4 cohorts: DOX, PAESe, DOX + PAESe and saline control, $n=5$ animals/cohort. The goal was to examine the effect of PAESe (25 mg/kg) at mitigating the toxicity of a larger dose of DOX (12.5 mg/kg) day 0, followed by resumption of normal dosing, *i.e.*, 5 mg/kg for DOX and 10 mg/kg for PAESe. Treatment was administered by tail vein injection under light anesthesia (1–2% isoflurane). Mice were monitored every day for survival and signs of treatment-mediated toxicity such as bloody stool and reduced physical activity. A Kaplan-Meir plot was used to visualize survival data and a Log-rank (Mantel-Cox) test was used determine if treatment-mediated differences in survival were significant, $p<0.05$ (SigmaStat, v.3.11).

In vitro Cardioprotective Activity of PAESe

Cell Lines

The rat derived H9C2 cardiomyocyte cell line was obtained from American Type Culture Collection (Rockville, MD) and cultured in complete growth media containing Dulbecco's modified Eagle's medium (DMEM) media supplemented with 10% (v/v) FBS and 1% penicillin and streptomycin antibiotics. Cells were grown in a humidified cell culture chamber at 37°C, 10% CO_2 and passaged at 70% confluency.

Reactive Oxygen Species (ROS)

DOX induced ROS measurements were carried out using BD Accuri C6 flow cytometer and data analysis completed using FlowJo software, v. 9.7.4. (Tree Start Inc., Ashland, OR). Cardiomyocytes were incubated with increasing concentrations of DOX (1, 10 and 50 μM), in presence of 1 μM PAESe for 24 h. Cells were then treated with 2′-7′-dichlorodihydrofluorescein diacetate (H_2DCFDA) (Molecular Probes) and washed after 30 min with PBS (12, 24). Cells were then lifted mechanically, rinsed with PBS and centrifuged for 5 min (1,000×*g*). Pellets were collected and resuspended in PBS. Approximately 10,000 cells were selected and subjected to fluorescence activated cell analysis at a wavelength 495 nm excitation and 520 nm emission. As a positive control, peroxide treated cells were measured. Data were normalized and then analyzed using a one-way ANOVA followed by a post hoc Bonferroni (all pair-wise comparisons) using (SigmaStat, v.3.11). Differences were considered significant at $p<0.05$.

Gene Expression, qPCR

Changes in expression of genes associated with DOX-mediated cardiac hypertrophy were measured by two-step quantitative polymerase chain reaction (qPCR) analysis in H9C2 cardiomyocytes treated with DOX (10 μM) for 2 h in the presence or absence of PAESe (0.5 and 1 μM) for 1 h followed by 24 h of growth media. A Qiagen RNAeasy mini kit (Germantown, MD) was used to isolate mRNA from cultured cardiomyocytes and converted to cDNA using a Bio-Rad iScript cDNA synthesis kit (Hercules, CA). QPCR SYBER Green Mix (Abgene) was used to conduct q-PCR analysis and standardized to β-actin. Primers for atrial natriuretic peptide (*ANP*), myosin heavy chain (*MHC-β*) and *β*-actin (housekeeping gene) have previously been constructed for rats and been measured in rat hearts as well as in H9C2 cardiomyocytes (25). The data were analyzed using the ΔΔCt method (24). As a positive control, peroxide treated cells were measured. Data were normalized were analyzed using a one-way ANOVA followed by a post hoc Bonferroni using (SigmaStat, v.3.11). Differences were considered significant at $p<0.05$.

In Vitro Cardiac Hypertrophy

H9C2 cells were plated onto glass coverslips, as indicated above. Cells were exposed to 2 μM DOX for 2 h followed by further incubation in fresh media for further 24 h. Cells were fixed with 4% (w/v) PBS-buffered formaldehyde and

incubated with rhodamine-conjugated phalloidin (Molecular Probes). Micrographs were acquired (10/slide) using a Nikon TiS inverted fluorescence microscope. Two blinded investigators assessed changes in morphometric size measurements from four independent experiments. A minimum of 200 cells per group were analyzed for differences in cell size. Changes in morphometric size were based upon fold change from control to treated cells. Differences in size were analyzed by ANOVA followed by a post hoc Bonferroni (all pair-wise comparisons) using (SigmaStat, v.3.11); a $p<0.05$ was considered significant.

RESULTS

Plasma Pharmacokinetics

The pharmacokinetics of free and liposome encapsulated PAESe were determined in Fisher 344 rats by LC-MS/MS; the description and validation of the assay is provided in ***supplemental data***. Free PAESe (10 mg/kg) or SSL-PAESe (5 mg/kg) was administered to rats as an *i.v.* bolus. Blood was collected over the next 4 h for free PAESe and 120 h for SSL-PAESe on the basis of pharmacokinetic differences between the two formulations. A noncompartmental analysis was used to estimate PK parameters and provide initial estimates for computational modeling. A two-compartment pharmacokinetic model with linear and stationary kinetics was chosen to provide the best fit of the observed plasma drug concentration–time data (Fig. 2) and used to estimate PK parameters (Table I).

These data showed the disposition of PAESe was changed significantly when encapsulated in SSL compared to free drug. Free PAESe was cleared rapidly from blood after *i.v.* administration with a rapid distribution half-life ($\alpha_{t1/2}$) of 1.96 min and an elimination half-life ($\beta_{t1/2}$) of 8.78 min. The apparent volume of distribution for free PAESe group was large (3.16 L/kg) relative to SSL-PAESe (0.502 L/kg), suggesting free PAESe distributes to tissues greater than SSL-PAESe (13, 26, 27). The circulation time was increased significantly in animals dosed with SSL-PAESe (101 h) compared to free PAESe (8.78 min). Total systemic CL was also decreased (−99.3%) significantly ($p<0.05$) and dose normalized AUC was increased (137%) significantly ($p<0.05$) in animals receiving SSL-PAESe compared to free PAESe. At the dose levels tested there was no evidence of obvious physical toxicity associated with either treatment group.

In Vivo Activity

Tumor volume and body weight are presented for 8 weeks after initiating treatment, Fig. 3. The tumor volumes of animals treated with DOX + PAESe, SSL-PAESe and DOX + SSL-PAESe groups were decreased significantly relative to control at 1 week after the last treatment, Fig. 3a. Free- and SSL-PAESe did not reduce DOX antitumor activity significantly, when administered concomitantly, DOX + PAESe (229%±20); DOX+SSL-PAESe (199%±41) compared to DOX (337%±46). A significant inhibition in tumor growth was observed initially on day 33 in the DOX + PAESe and DOX+SSL-PAESe groups, and surprisingly the SSL-PAESe group (309%±63) compared to the saline treated controls (786%±234). It should be noted that the dose used for SSL-PAESe group was 5 mg/kg, which was half the dose of PAESe used in PAESe free drug treatment group (10 mg/kg).

As shown in Fig. 3b, body weight of DOX (5%±5) and DOX + PAESe (3%±6) groups were significantly lower than PAESe (25%±2) and SSL-PAESe (25%±2) groups from day 51. A significant difference in body weight between control (12%±4) and DOX+SSL-PAESe (11%±5) groups was not observed, relative to PAESe and SSL-PAESe.

More importantly, the survival of mice in the SSL-PAESe and DOX+SSL-PAESe groups were increased significantly compared to animals receiving saline and DOX, as shown in Fig. 4a. The median survival for control (day 55) and DOX

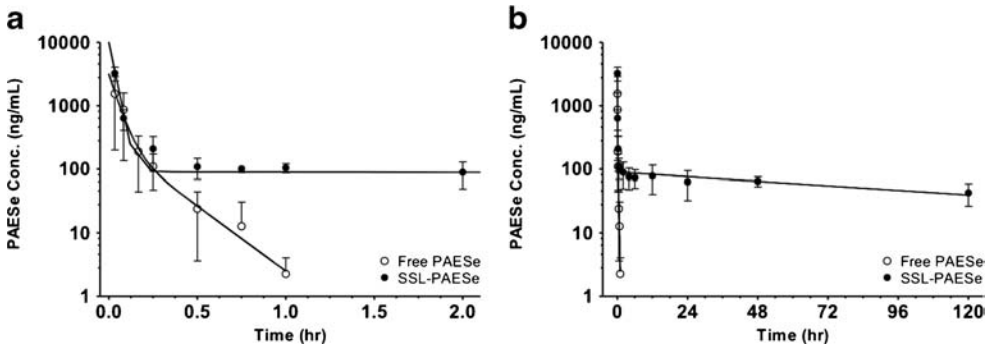

Fig. 2 Plasma concentration-time profile of free PAESe and SSL-PAESe. Free PAESe (10 mg/kg) and SSL-PAESe (5 mg/kg) were administered intravenously into rats, panel (**a**) shows 0–2 h and (**b**) shows 0–120 h. Blood samples (100–200 μL) were collected *via* a jugular cannula. Plasma was separated from blood by centrifugation at 1,200 × *g* for 10 min at 4°C and was analyzed by LC-MS/MS. Data is presented as means ± standard deviation of two independent studies ($n=4$ for free PAESe; $n=6$ for SSL-PAESe), lines represent model fit of mean data.

Table I Model-Predicted Pharmacokinetic Parameters for Free PAESe and SSL-PAESe

Variables	Free PAESe Mean (CV %)	SSL-PAESe Mean (CV %)
Dose (mg/kg)	10	5
Distribution half-life, $\alpha_{t1/2}$ (hr)	0.0326 (31.0)	0.0201 (19.5)
Elimination half-life, $\beta_{t1/2}$ (hr)	0.146 (13.3)	101 (30.2)*
AUC ($\mu g \bullet$hr/mL)	0.196 (17.8)	13.5 (26.3)*
AUC/Dose ($\mu g \bullet$hr/mL/kg)	0.0196	2.70
Volume of distribution, V (L/kg)	3.16 (38.2)	0.502 (40.8)*
Total Clearance, CL (L/hr/kg)	51.2 (17.8)	0.371 (26.3)*

AUC area under drug concentration time profile. *$p < 0.05$

group (day 58) were not significantly different (Table II), even though the tumor volume of DOX group was smaller ($p<0.05$) relative to the control group, suggesting that the toxicity of DOX may contribute to the decreased survival of animals, whereas control groups had shorter survival time due to tumor burden and disease progression. However, concomitant use of DOX with PAESe (DOX + PAESe; day 75) or SSL-PAESe (DOX+SSL-PAESe; day 72) did extend survival compared with the DOX treatment group (day 58), while tumor volume of these combination groups were not significantly different relative to that of the DOX group (Fig. 3a). Further, the median survival was not different significantly among the groups treated with DOX + PAESe (day 75), DOX+SSL-PAESe (day 72) and PAESe (day 71). Notably, the survival time for SSL-PAESe group in the absence of DOX, was increased significantly compared to control and DOX group (Fig. 4a and Table II). The median survival was increased by 62% for SSL-PAESe group relative to controls and 53% relative to DOX groups (Table II).

Morphometric analysis of cardiomyocytes from representative views across the heart suggested PAESe decreases cardiac hypertrophy associated with DOX treatment (Fig. 4b). DOX treatment resulted in a significant increase (20%) in cross sectional width of cardiomyocytes, where PAESe and DOX + PAESe were not significant from control. Interestingly, SSL-PAESe and DOX + SSL-PAESe had 7 to 8% decreases in size that were also significant.

Greater DOX Dosing

The ability of PAESe to mitigate toxicity associated with increased DOX dosing was determined in healthy, non-tumor bearing NCr mice. Administration of DOX at 12.5 mg/kg (high dose) resulted in significant toxicity in the DOX treatment group (Fig. 5). It should be noted that immediately after administration two mice exhibited severe toxicity (1 died and 1 required euthanasia) and they were excluded from the Kaplan Meir-Plot and statistical analysis. Two weeks after initiation of this study a total of 33% of DOX, 80% of DOX + PAESe and 100% of PAESe or control mice were alive. The study was terminated at 21 days as a result of the toxicity to DOX treated group. Significant ($p<0.05$) differences in the survival of the DOX and DOX + PAESe, PAESe or control treatment groups were observed. The survival of mice treated with DOX + PAESe was not significantly different compared to the PAESe and control groups.

Reactive Oxygen Species

Our data confirm previous findings indicating that greater concentrations of DOX increased ROS formation in cardiomyocytes (Fig. 6) (24). Further we demonstrated that PAESe (1 μM) reduced DOX mediated ROS formation by 1.84 and 1.62 fold, following incubation with 10 and 50 μM DOX, respectively, as measured by flow cytometry analysis utilizing H_2DCFDA, (Fig. 6).

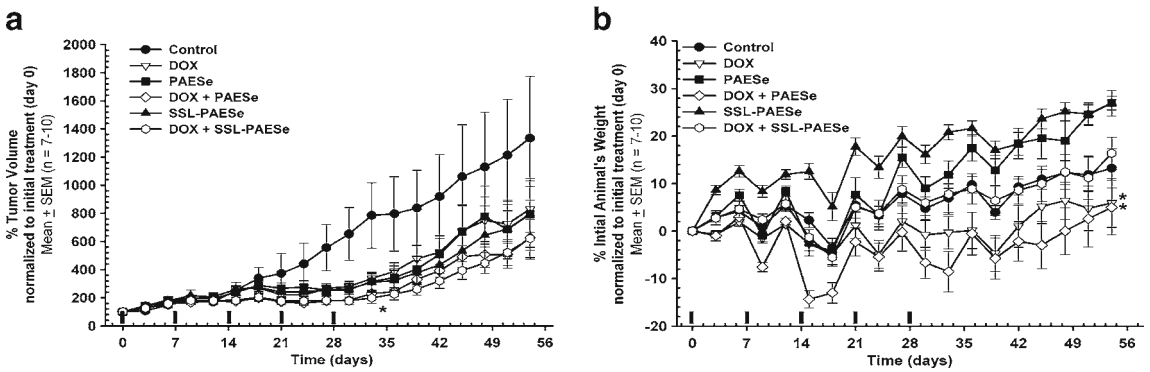

Fig. 3 Effect of SSL-PAESe on tumor growth (**a**) and body weight (**b**) in a PC-3 xenograft model. The effect of encapsulated PAESe in long circulating liposome (SSL-PAESe) on tumor growth (**a**) and body weight (**b**) was determined in a tumor (PC-3) xenograft mouse model. After tumors reached 200 mm^3, treatment was initiated with 5 mg/kg/week for DOX and 10 mg/kg/week for PAESe, and 5 mg/kg/week for SSL-PAESe by tail vein injection (*solid rectangular bars*) weekly. Tumor volume and body weight were monitored every 3 days, data are presented as means ± SEM ($n = 8–10$) and were normalized to average tumor volume or body weight on day 0. An *asterisk* indicates a significant ($p < 0.05$) difference compared to control; panel (**a**), Lip-PAESe + DOX and DOX + PAESe.

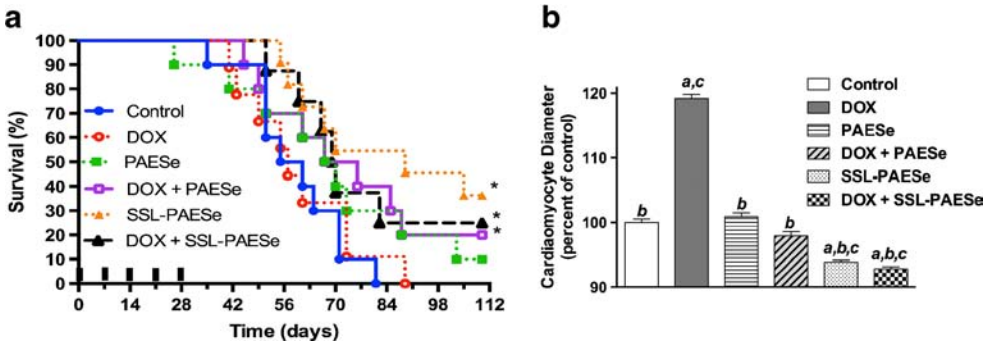

Fig. 4 PAESe improves survival and reduces cardiac hypertrophy. The effect of SSL-PAESe on survival was determined in a tumor (PC-3) xenograft mouse model. (**a**) After tumors reached 200 mm^3, treatment was initiated with 5 mg/kg/week for DOX and 10 mg/kg/week for PAESe, and 5 mg/kg/week for SSL-PAESe by tail vein injection weekly (solid rectangular bars). A Log-rank (Mantel-Cox) test was used determine if treatment-mediated differences in survival were significant relative to control; $^*p < 0.05$. (**b**) The effect of treatment on cardiac hypertrophy was determined. Mean ± SEM ($n = 225$/heart × 9–12 hearts), where = $p \leq 0.05$ [a]relative to control, [b]relative to DOX and [c]relative to PAESe.

Gene Expression

Previously it has been shown that DOX mediated ROS formation induced cardiac hypertrophy (28, 29). Our data verify that DOX (10 μM) induces the development of cardiac hypertrophy by measuring changes in markers (gene expression) associated with the development of cardiac hypertrophy such as *ANP* (3.34 fold increase *vs.* control) and *MHC-β*, (2.34 fold increase *vs.* control). Use of PAESe (1 μM) reduced DOX-mediated increases in the expression of *ANP* by 3.2 fold and *MHC-β* by 2.2 fold. To further assess the cardioprotective effects of PAESe against DOX mediated cardiac hypertrophy we measured morphometric size, Fig. 8. Concomitant use with PAESe (1 μM) reduced DOX (10 μM) mediated increases in cardiomyocyte size by approximately 60%.

DISCUSSION

Failure to achieve optimal chemotherapeutic exposure can lead to disease progression, drug resistance and death (30). Anthracyclines, including DOX, are used widely in various treatment schedules for primary and metastatic cancers, however dose-limiting cardiotoxicity limits their overall use. The use of anthracyclines has been associated with formation of reactive free radicals species (ROS), development of cardiac hypertrophy, cardiac myopathy and death. The specific molecular targets and time-course of events leading to acute and chronic cardiotoxicities are still largely unknown. Various strategies including coadministration of antioxidants have been examined to mitigate DOX-mediated cardiotoxicity, but none are highly effective. Dexrazoxane is one such antioxidant that is approved by FDA to mitigate DOX-mitigated cardiotoxicity, but it has been shown to reduce the antitumor effect of DOX or have off target toxicities. Therefore, discovery and development of new cardioprotective approaches are needed.

Selenium is an essential component of selenocysteine, the active site of glutathione peroxidase (GSHPx) (31, 32). GSHPx is a well-established antioxidant enzyme that decreases oxidant-induced DNA damages and lipid

Table II Treatment Mediated Survival

	Median days survival (Range)	% Increase in median survival *vs.* control	*p* value
Control	55 (35–81)	–	–
DOX	58 (41–89)	5	0.1765
PAESe	71 (26 – N/A)	29	0.0144
DOX + PAESe	75 (45 – N/A)	36	0.0021
SSL-PAESe	89 (55 – N/A)	62	0.0005
DOX + SSL-PAESe	72 (52 – N/A)	31	0.0006

p value: From statistical analysis of each group *vs.* control using Kaplan-Meier analysis and a Log-rank (Mantel-Cox) test

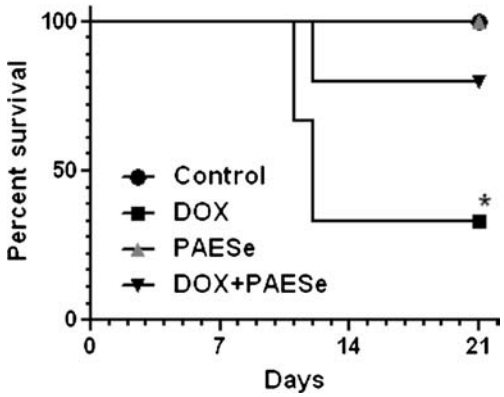

Fig. 5 Effect of PAESe on High Dose DOX. The effect of PAESe on survival was determined in health mice. Mice were treated initially (day 0) with high DOX (12.5 mg/kg), PAESe (25 mg/kg), DOX + PAESe (12.5 and 25 mg/kg, respectively) or saline, and then weekly (day 7 and 14) with DOX (5 mg/kg), PAESe (10 mg/kg), DOX + PAESe (5 and 10 mg/kg, respectively) or saline. A Log-rank (Mantel-Cox) test was used to determine if treatment-mediated differences in survival were significant relative to control; $^*p < 0.05$.

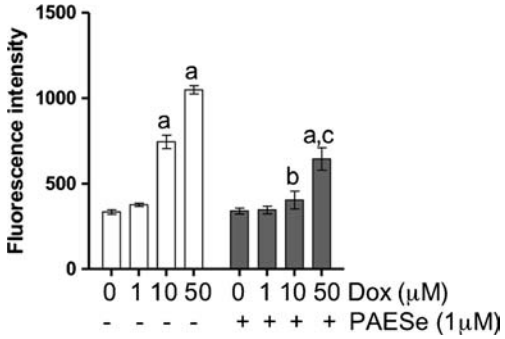

Fig. 6 PAESe attenuates DOX mediated ROS formation. PAESe (1.0 μM) reduces DOX (1, 10 and 50 μM) mediated ROS formation as determined by flow cytometry using H_2DCFDA. Mean ± SEM ($n = 6$ independent studies), where = $p \leq 0.05$ [a]relative to control, [b]relative to 10 μM DOX and [c]relative to 50 μM DOX.

peroxidation caused by oxidation, and is highly correlated with the initiation and progression of malignancy (31, 33). Other studies have shown that selenium has antiangiogenic activity *in vitro* and *in vivo* through inducing apoptosis and regulating matrix metalloproteinase activity and vascular endothelial growth factor levels (34). However, many studies have used antioxidants, including free selenium, to reduce ROS generation in cell models, however these results have not translated well into laboratory animal models or human clinical trials. Specifically, free selenium did not show a significant protective effect against DOX-induced lethality associated with chronic cardiotoxicity (35). The reasons for these differences are not known, but we have shown incorporation of selenium into PAESe appear to mediate alterations in expression of genes that have been correlated to cardiotoxicity in addition to its direct antioxidant effects.

PAESe is a phenylaminoalkyl selenide and potent antioxidant that exhibits antihypertensive activity mediated by a scavenging effect of reactive oxygen species, which is associated with dopamine-β-monooxygenase dependent ascorbate depletion and regeneration of glutathione (10, 11, 36). Moreover, a remarkable property of this compound is that the selenoxide product generated from their antioxidant activity are readily recycled back to its selenide form by cellular reductants such as ascorbate and glutathione (10, 11, 36). Further, we have shown that these compounds are stable in cell culture, have very low toxicity *in vivo* (rats and mice), and react stoichiometrically with oxidants to form the selenoxide products with no complicating side reactions. Recently, we demonstrated that PAESe exhibits a protective effect against anthracycline-induced cardiotoxicity *in vitro* cell culture as well as *in vivo* antitumor activity (12).

Here, we developed and used an LC–MS/MS assay to quantify the PK of free PAESe and SSL-PAESe. Free PAESe was eliminated rapidly and was not detectable at 1 h after administration. Contrary to free drug, PAESe was observed in the rat plasma for a prolonged period and detectable (42 ng/mL) up to 120 h after administration when encapsulated in liposomes, SSL-PAESe. Although the free fraction of PAESe was not determined explicitly, based on rapid clearance of free PAESe, it is supportive that PAESe was entrapped stably within the SSL. This is similar to other drugs that are rapidly cleared when compared to those remote-loaded into SSL formulations (13, 15). The difference in concentration-time profile of free *versus* SSL-PAESe provides an opportunity to examine the effect of drug exposure on its pharmacological activity.

PAESe decreased tumor volume without altering the antitumor activity of DOX, while exhibiting both acute and chronic cardioprotective activity using a human prostate cancer xenograft mouse model. It is noteworthy that tumor volume was decreased significantly by day 33 in DOX + PAESe, SSL-PAESe, and DOX+SSL-PAESe groups compared to control group even though the dose of PAESe in the SSL-PAESe formulations was half of the free PAESe. Survival data also showed that groups treated with SSL-PAESe (with or without DOX) lived longer than other groups while tumor volume of these groups (SSL-PAESe and DOX+SSL-PAESe) were not significantly different relative to the DOX treatment group. Furthermore, the concomitant use of PAESe

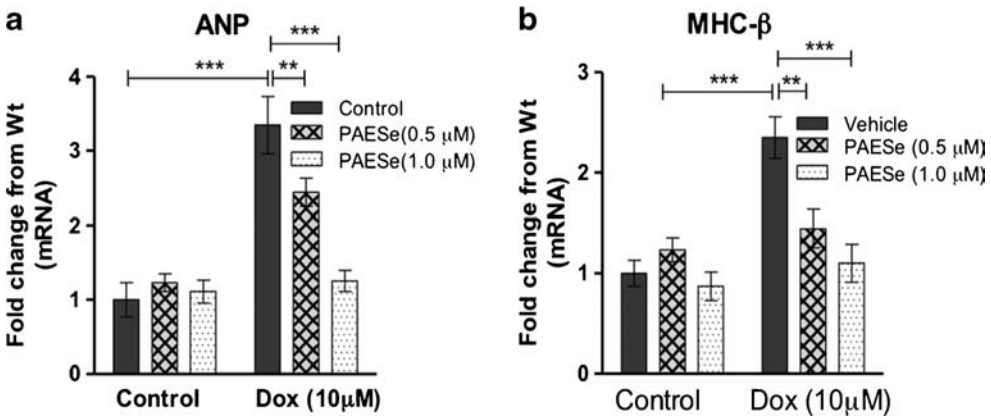

Fig. 7 PAESe inhibits DOX mediated markers for cardiac hypertrophy in H9C2 cardiomyocytes. PAESe (0.5 and 1.0 μM) prevents DOX mediated increase in markers associated with the development of cardiac hypertrophy (**a)** *ANP* and (**b**) *MHC-β*, as determined by two-step qPCR. Data are represented as fold change from control and standardized to β-actin. Where $n =$ 4 independent experiments. $^{**}p < 0.005$ and $^{***}p < 0.0001$ *vs.* control.

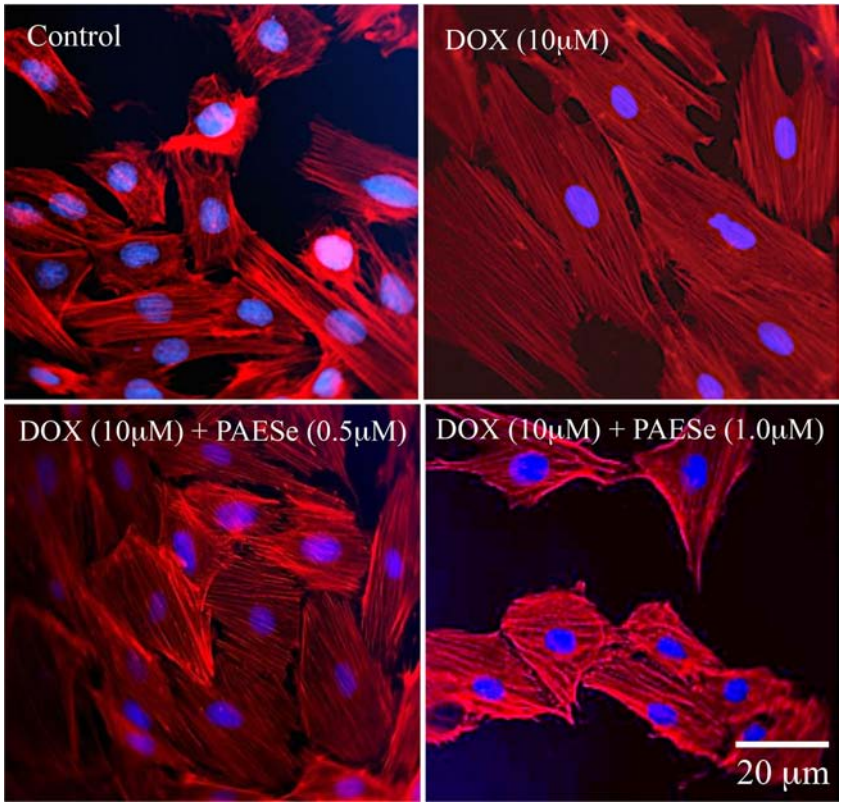

Fig. 8 PAESe inhibits DOX mediated cardiac hypertrophy in H9C2 cardiomyocytes. PAESe (0.5 and 1.0 μM) prevents DOX (10 μM) mediated increase in cardiac hypertrophy as measured by morphometric (size) analysis. Data is represented as fold change from control. Where $*p \leq 0.05$, $**p \leq 0.005$ *vs.* control, $n = 4$ studies.

resulted in enhanced survival and overall better appearance of the animals treated with a high dose (12.5 mg/kg) followed by conventional (5 mg/kg) dose of DOX in healthy mice in the presence and absence of free PAESe. Treatment mediated toxicity in DOX treated groups was observed immediately and throughout this study. These data suggest that PAESe may be used to better titrate DOX, however further studies are needed to examine treatment efficacy and toxicities.

Previously we examined the effect of DOX and PAESe on prostate cancer cells and showed reduction in ROS and improved survival (12). In this study mice treated with DOX and PAESe showed decreased evidence of cardiac hypertrophy, a precursor to cardiomyopathy and cardiac failure. In H9C2 cells the concomitant treatment with free PAESe (at 0.5 and 1.0 μM) significantly reduced DOX-mediated (10 μM) expression of *ANP* and *MHC-β*, makers of cardiac hypertrophy (Fig. 7). This correlated with changes in morphometric size analysis of cardiomyocytes (Fig. 8). These and previous data suggest that PAESe may be mediating both acute antioxidant activity *via* its ability to rapidly scavenge reactive oxygen species and regenerate glutathione and ascorbate stores, and offer long term protection by protecting against expression of genes and development of cardiac hypertrophy. Elucidation of the underlying mechanisms may allow these and other genes associated with cardiotoxicity to serve biomarkers to examine novel dosing schedules or treatment mediated effects.

The improved survival and reduced cardiac hypertrophy following the concomitant use of PAES has the potential to provide oncologists greater flexibility when treating patients with DOX. Although clinical use of Dexrazoxane is not optimal it is used widely and been shown to reduce cardiotoxicity. Additional studies are needed to examine the concomitant use of Dexrazoxane and PAESe with DOX and other agents that have been shown to exhibit cardiotoxicity. Dexrazoxane's ability to reduced generation of ROS combined with PAESe direct antitumor activity to scavenge ROS, regenerate glutathione peroxidase, and alter gene expression may further improve cardioprotection and antitumor activity following treatment with DOX.

In conclusion, free- and SSL-PAESe were shown to have direct *in vivo* antitumor activity and did not mitigate DOX antitumor activity. PAESe also was shown to be cardioprotective, reduce cardiac hypertrophy and prolong survival in a tumor xenograft and high-dose DOX treatment animal models.

ACKNOWLEDGMENTS AND DISCLOSURES

This research was funded in part by NIH 1R01 1EB016100-01 and 1R21 EB008153 (RDA), Auburn University Internal Grants Program, Georgia Cancer Coalition Distinguished Scholar Grant (RDA) and University of Georgia-Georgia Tech Seed Grant (SWM/RDA).

REFERENCES

1. Hande f. Clinical applications of anticancer drugs targeted to topoisomerase II. Biochim et Biophys Acta (BBA) Gene Struct Expr. 1998;1400(1,Äì3):173–84.
2. Quiles JL, Huertas JR, Battino M, Mataix J, Ramirez-Tortosa MC. Antioxidant nutrients and adriamycin toxicity. Toxicology. 2002;180:79–95.
3. Minotti G, Menna P, Salvatorelli E, Cairo G, Gianni L. Anthracyclines: molecular advances and pharmacologic developments in antitumor activity and cardiotoxicity. Pharmacol Rev. 2004;56(2):185–229.
4. Herman EH, Zhang J, Chadwick DP, Ferrans VJ. Comparison of the protective effects of amifostine and dexrazoxane against the toxicity of doxorubicin in spontaneously hypertensive rats. Cancer Chemother Pharmacol. 2000;45(4):329–34.
5. Pearlman M, Jendiroba D, Pagliaro L, Keyhani A, Liu B, Freireich EJ. Dexrazoxane in combination with anthracyclines lead to a synergistic cytotoxic response in acute myelogenous leukemia cell lines. Leuk Res. 2003;27(7):617–26.
6. Spencer CM, Goa KL. Amifostine. A review of its pharmacodynamic and pharmacokinetic properties, and therapeutic potential as a radioprotector and cytotoxic chemoprotector. Drugs. 1995;50(6): 1001–31.
7. Treskes M, van der Vijgh WJ. WR2721 as a modulator of cisplatin- and carboplatin-induced side effects in comparison with other chemoprotective agents: a molecular approach. Cancer Chemother Pharmacol. 1993;33(2):93–106.
8. May SW. Selenium-based drug design: rationale and therapeutic potential. Expert Opin Investig Drugs. 1999;8(7):1017–30.
9. May SW. Selenium-based pharmacological agents: an update. Expert Opin Investig Drugs. 2002;11(9):1261–9.
10. May SW, Pollock SH. Selenium-based antihypertensives: rationale and potential. Drugs. 1998;56:959–64.
11. May SW, Wang L, Gill-Woznichak MM, Browner RF, Ogonowski AA, Smith JB, *et al.* An orally active selenium-based antihypertensive agent with restricted CNS permeability. J Pharmacol Exp Ther. 1997;283(2):470–7.
12. Kang JY, Costyn LJ, Nagy T, Cowan EA, Oldham CD, May SW, *et al*. The antioxidant phenylaminoethyl selenide reduces doxorubicin-induced cardiotoxicity in a xenograft model of human prostate cancer. Arch Biochem Biophys. 2011;515:112–9.
13. Arnold RD, Mager DE, Slack JE, Straubinger RM. Effect of repetitive administration of Doxorubicin-containing liposomes on plasma pharmacokinetics and drug biodistribution in a rat brain tumor model. Clin Cancer Res. 2005;11(24 Pt 1):8856–65.
14. Siegal T, Horowitz A, Gabizon A. Doxorubicin encapsulated in sterically stabilized liposomes for the treatment of a brain tumor model: biodistribution and therapeutic efficacy. J Neurosurg. 1995;83(6):1029–37.
15. Gabizon A, Shiota R, Papahadjopoulos D. Pharmacokinetics and tissue distribution of doxorubicin encapsulated in stable liposomes with long circulation times. J Natl Cancer Inst. 1989;81(19):1484–8.
16. Sharma US, Sharma A, Chau RI, Straubinger RM. Liposome-mediated therapy of intracranial brain tumors in a rat model. Pharm Res. 1997;14(8):992–8.
17. Arnold RD, Slack JE, Straubinger RM. Quantification of Doxorubicin and metabolites in rat plasma and small volume tissue samples by liquid chromatography/electrospray tandem mass spectroscopy. J Chromatogr B. 2004;808(2):141–52.
18. Zhu G, Alhamhoom Y, Cummings BS, Arnold RD. Synthesis of lipids for development of multifunctional lipid-based drug-carriers. Bioorg Med Chem Lett. 2011;21:6370–5.
19. Zhu G, Mock JN, Aljuffali I, Cummings BS, Arnold RD. Secretory phospholipase A2 responsive liposomes. J Pharm Sci. 2011;100(8): 3146–59.
20. Bartlett GR. Phosphorous assay in column chromatography. J Biol Chem. 1959;234:466–8.
21. Gabrielsson J, Weiner D. Pharmacokinetic Pharmacodynamic Data Analysis: Concepts and Applications. 4th ed. Sweden: Swedish Pharmaceutical Press. 2007:438–63.
22. Davol PA, Frackelton AR. Targeting human prostatic carcinoma through basic fibroblast growth factor receptors in an animal model: characterizing and circumventing mechanisms of tumor resistance. Prostate. 1999;40(3):178–91.
23. Wong HL, Rauth AM, Bendayan R, Wu XY. In vivo evaluation of a new polymer-lipid hybrid nanoparticle (PLN) formulation of doxorubicin in a murine solid tumor model. Eur J Pharm Biopharm Off J Arbeitsgemeinschaft fur Pharm Verfahrenstechnik eV. 2007;65(3): 300–8.
24. Nanayakkara G, Viswaprakash N, Zhong J, Kariharan T, Quindry J, Amin R. PPARgamma activation improves the molecular and functional components of I(to) remodeling by angiotensin II. Curr Pharm Des. 2013;19(27):4839–47.
25. Karagiannis TC, Lin A, Ververis K, Chang L, Tang MM, Okabe J, *et al.* Trichostatin A accentuates doxorubicin-induced hypertrophy in cardiac myocytes. Aging (Albany NY). 2010;2(10):659–68.
26. MacKichan JJ. Influence of protein binding and use of unbound (free) drug concentrations. Applied Pharmacokinetics. Vancouver, Washington: Applied Therapeutics; 1992. p. 1–48.
27. McNamara PJ, Levy G, Gibaldi M. Effect of plasma protein and tissue binding on the time course of drug concentration in plasma. J Pharmacokinet Biopharm. 1979;7(2): 195–206.
28. Hunter JJ, Chien KR. Signaling pathways for cardiac hypertrophy and failure. N Engl J Med. 1999;341(17):1276–83.
29. Sardao VA, Oliveira PJ, Holy J, Oliveira CR, Wallace KB. Morphological alterations induced by doxorubicin on H9c2 myoblasts: nuclear, mitochondrial, and cytoskeletal targets. Cell Biol Toxicol. 2009;25(3):227–43.
30. Straubinger RM, Arnold RD, Zhou R, Mazurchuk R, Slack JE. Antivascular and antitumor activities of liposome-associated drugs. Anticancer Res. 2004;24(2A):397–404.
31. Ursini F, Bindoli A. The role of selenium peroxidases in the protection against oxidative damage of membranes. Chem Phys Lipids. 1987;44(2–4):255–76.
32. Gladyshev VN, Jeang KT, Stadtman TC. Selenocysteine, identified as the penultimate C-terminal residue in human T-cell thioredoxin reductase, corresponds to TGA in the human placental gene. Proc Natl Acad Sci U S A. 1996;93(12):6146–51.
33. Sundstrom H, Korpela H, Viinikka L, Kauppila A. Serum selenium and glutathione peroxidase, and plasma lipid peroxides in uterine, ovarian or vulvar cancer, and their responses to antioxidants in patients with ovarian cancer. Cancer Lett. 1984;24(1):1–10.
34. Jiang C, Jiang W, Ip C, Ganther H, Lu J. Selenium-induced inhibition of angiogenesis in mammary cancer at chemopreventive levels of intake. Mol Carcinog. 1999;26(4):213–25.
35. Hermansen K, Wassermann K. The effect of vitamin E and selenium on doxorubicin (Adriamycin) induced delayed toxicity in mice. Acta Pharmacol Toxicol. 1986;58(1):31–7.
36. May SW, Herman HH, Roberts SF, Ciccarello MC. Ascorbate depletion as a consequence of product recycling during dopamine.beta.-monooxygenase catalyzed selenoxidation. Biochemistry. 1987;26(6):1626–33.